Step-Size Adaptation Based on Power and Current Variation for Photovoltaic Maximum-Power-Point Tracking

Peeradech Lousuwankun[1] and Niphat Jantharamin[1,*]

ARTICLE INFO

Article history:
Received: 7 June 2021
Revised: 1 July 2021
Accepted: 9 July 2021

Keywords:
Step-size adaptation
Photovoltaic
Maximum power point
Incremental conductance

ABSTRACT

This study presents a step-size adaptation technique for power maximization of photovoltaic (PV) arrays. Since a PV array generates optimal power output when operating at the maximum power point (MPP), the approach of maximum power point tracking (MPPT) is incorporated to regulate the array terminal voltage in such a way that the array output power is always maximized. Hereby, the change in the array voltage refers to the step size in the MPPT algorithm. The adaptive step size is subject to the array operating point location related to the existent MPP. In the purposed technique, determination of the desired step size is based on alteration of the array power and current. The MPPT task was performed by means of a step-up converter, in which the duty ratio adaptation is established in connection with the intended step size and the tracking direction is determined by the incremental conductance algorithm. During MPPT implementation, the converter duty ratio is progressively changed, and therefore higher tracking speed and reduction of steady-state fluctuation in the vicinity of the MPP can be achieved. Moreover, the purposed technique is independent of PV array specification, and hence can be applied to any PV arrays without prior test or simulation. The proposed step-size adaptation provided superior MPPT performance under fast fluctuations in weather condition, by comparison with the multiplier-based step-size adaptation and the fixed step-size strategy.

1. INTRODUCTION

An uninterrupted increase in growth rate of world population causes a continual rise of yearly energy consumption. Worldwide energy demand has been dominated by fossil fuels-i.e. coal, crude oil, and natural gas. Combustion of these fuels generates carbon dioxide, and results in higher atmospheric concentration of carbon dioxide that creates the biggest influence on global warming. The substantial rise in energy demand also causes a quick reduction of these fuel reserves. Following the environmental problem as well as an increasing agitation about insufficiency of traditional energy reserves, renewable energy sources have recently received more attention. Among these energy types, solar energy is accessible everywhere, and has been considered more than sufficient for the annual worldwide energy consumption [1]. Therefore, the energy from sunlight has presented its possibility for being an alternative energy source, and becomes a promising solution for electrification of remote areas. Direct conversion of solar energy into electricity can be realized by means of a photovoltaic (PV) module. Based on its modular structure, the modules can be connected to form a PV array to increase PV output power: series connection of the modules increases the output voltage whereas parallel connection of the modules results in higher output current.

PV arrays have no moving components, need no fuel, and work without generating air pollution and noise. Therefore, the arrays are nearly free of maintenance and environmentally amicable. However, the PV array output power relies directly on weather conditions. The array short-circuit current, which is equal to the photocurrent produced in the array, changes linearly with the intensity of incident sunlight. On the other hand, the array open-circuit voltage changes logarithmically with the irradiance. In accordance with lower irradiance, the array power evidently drops as indicated in Fig. 1. While the temperature of solar cell increases, the open-circuit voltage falls nearly linearly as the photocurrent rises marginally. Since this unfavorable effect of solar cell temperature on the open-circuit voltage is dominant in comparison with the increased short-circuit current, the array power therefore decreases with higher solar cell temperature as presented in Fig. 2.

[1]*Department of Electrical and Computer Engineering, Faculty of Engineering, Naresuan University, Phitsanulok, 56000, Thailand*.
**Corresponding author:* Niphat Jantharamin; Phone: +66-55-964-390; Email: niphatj@nu.ac.th.

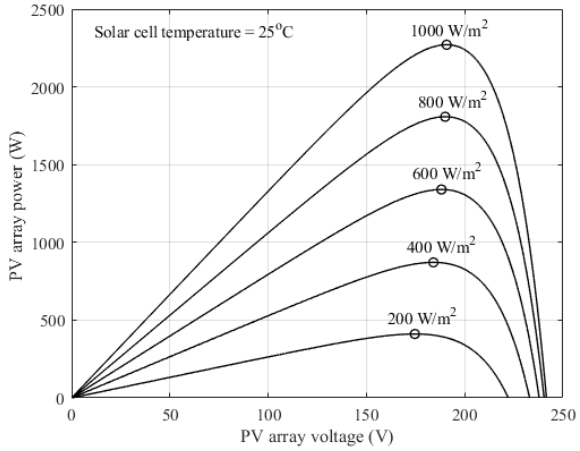

Fig. 1. Irradiance effect on PV array power-voltage curves.

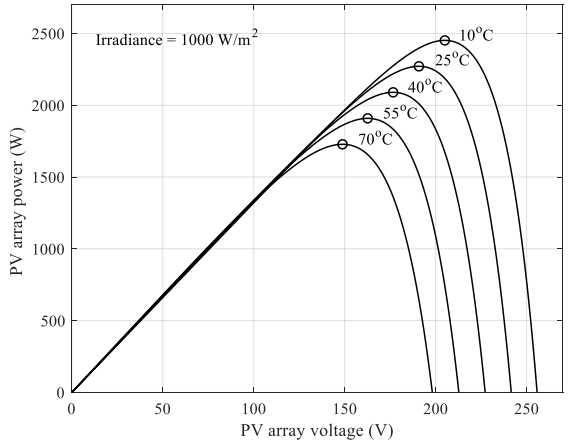

Fig. 2. Solar cell temperature effect on PV array power-voltage curves.

Regarding the PV array output characteristics, the operating point where the array deliver maximum power is called the maximum power point (MPP). The MPP position depends directly on environmental fluctuation, which corresponds to geological regions, seasons, and day time. Lower incident light intensity and higher solar cell temperature tends to cause the MPP to be located at a lower voltage. However, the array operating point has to be placed at the MPP to maximize the array output power. In accordance with a specific environmental condition, the array voltage must be regulated in such a way that the array output power maximization is accomplished, which can be realized by including the maximum-power-point tracking (MPPT) algorithm.

2. MAXIMUM-POWER-POINT TRACKING

Various techniques for MPPT, each of which possesses benefits and restrictions, have been presented in the literature. None of these techniques is appropriate for all MPPT usages. Normally, the circuitry and algorithm simplicity, tracking accuracy and speed, cost of controller, obtainable data and user expertise are significant aspects for decisiveness. Some of these methods rely on the nearly linear correlation between the MPP and the solar-cell open-circuit voltage and short-circuit current [2]. Even though these methods are cost-effective and straightforward to implement, determination of optimum proportional coefficients is exhausting and time-consuming, and the measurement of open-circuit voltage and short-circuit current results in power loss since the usual system performance is interfered. In addition, neural networks and fuzzy logic control have recently become a significant part in MPPT due to their handling competence of system nonlinearity. The fuzzy logic control is capable of coping inaccurate inputs and needs no precise model. Furthermore, the neural network is able to develop a connection between any kind of input and output data, providing that information for network training is obtainable [3]. Controller credibility and technique accuracy rely however directly on the user proficiency.

In reality, the perturb-and-observe (P&O) technique has been most generally applied for MPPT due to algorithm simplicity and no prior knowledge requirement of the array. The array power is observed while the array voltage is perturbed. Comparison of the power value with its former value at the previous sampling determines the next step direction [4]. Steady-state fluctuation of the array operating point in the vicinity of the MPP however refers to power loss, which can be reduced by using smaller step size in exchange for slower tracking speed. The technique also loses tracking direction under continuously rapid change in irradiance. On the other hand, the incremental conductance technique can successfully handle MPPT under quick irradiance variation, and was therefore adopted for MPPT in this research. The algorithm of the incremental conductance technique is described in Fig.3. This method relies on the slope of the power-voltage curve of the array. On the left side and on the right side of the MPP, the slope is positive and negative respectively. the slope becomes zero at the MPP. Following the comparison between the incremental conductance ($\Delta I_{pv}/\Delta V_{pv}$) and the instantaneous conductance (I_{pv}/V_{pv}), the location of the operating point related to the MPP is determined, and the proper tracking direction is indicated. The conditional expressions according to the incremental conductance technique are as follows:

$$\frac{\Delta I_{pv}}{\Delta V_{pv}} < -\frac{I_{pv}}{V_{pv}} \text{ on the right side of the MPP,}$$

$$\frac{\Delta I_{pv}}{\Delta V_{pv}} > -\frac{I_{pv}}{V_{pv}} \text{ on the left side of the MPP, and}$$

$$\frac{\Delta I_{pv}}{\Delta V_{pv}} = -\frac{I_{pv}}{V_{pv}} \text{ at the MPP.}$$

Perturbation of the PV array voltage (V_{pv}) depends on the array operating point position relative to the MPP. V_{pv} is reduced when the array operating point is located on the right side of the MPP. However, V_{pv} is raised as the array operating point is located on the left side of the MPP. After reaching the MPP, V_{pv} is held constant to keep operating at this point until the PV array current changes [5].

Moving the array operating point typically uses fixed step-size scheme, by which a chosen fixed step size strongly affects MPPT performance. Using a big step size can reduce tracking time but causes the array operating point to oscillate around the MPP at steady state. On the contrary, using a small step size can slow down the tracking speed, despite elimination of the oscillation. To improve the tracking speed and avoid the steady-state fluctuation, an adaptive step-size scheme is more desirable: a big step size is used while the MPP is far, and the step size becomes smaller when the MPP is close.

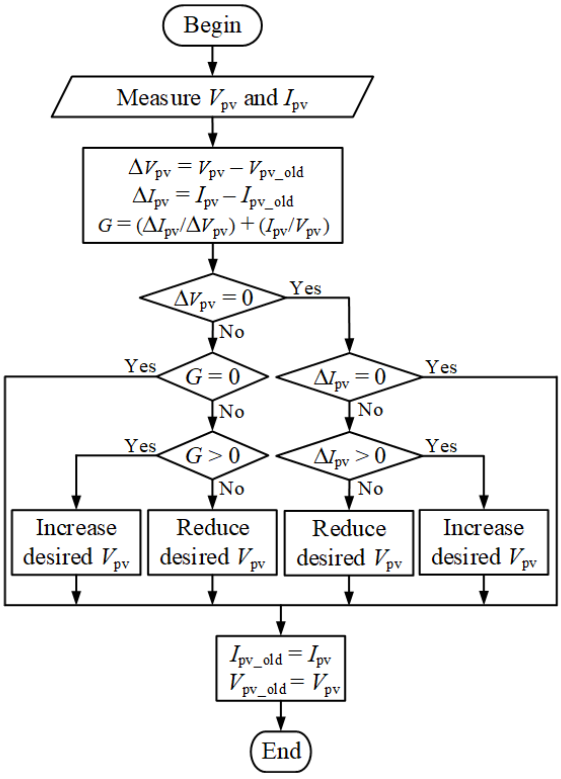

Fig. 3. Incremental conductance technique algorithm.

3. STEP-SIZE ADAPTATION BASED ON MULTIPLIERS

Apart from tracking speed improvement and steady-state oscillation elimination, the adaptive step-size scheme also alleviates failure to meet the MPP when the incremental conductance technique is used. The step size can be changed by multiplying the number 1 or 2 to a fixed step size relying on the array operating point location and the direction of perturbation. As getting closer to the MPP, a fixed step-size perturbation is applied. The step size is doubled when the perturbation is reversed providing that the array operating point departs from the MPP [6]. Another version of step-size adaptation with two multipliers introduces a high-value multiplier and a low-value multiplier to a fixed step size. These multipliers are specifically chosen for each PV array. Based on gradient magnitude, the array power-voltage curve is divided into regions, where each multiplier is used. Selection of too high multipliers can cause the operating point to jump over and oscillate around the MPP for a long time.

However, step-size adaptation with three multipliers-i.e. a low multiplier, a medium multiplier, and a high multiplier, can increase the tracking speed while alleviating the aforementioned problems. The region dividers for the three-multiplier scheme are defined as follows:

$$\sigma_L = \frac{1}{4} \cdot \left| \frac{dP}{dV} \right|_{\max} \quad (1)$$

$$\sigma_H = \frac{1}{2} \cdot \left| \frac{dP}{dV} \right|_{\max} \quad (2)$$

where, σ_L is a boundary of low gradient magnitude area, σ_H is a boundary of high gradient magnitude area on the power-voltage characteristic curve. $|dP/dV|_{\max}$ explains the maximum gradient magnitude of power-voltage characteristic curve of the considered PV array under the standard test conditions (STC) and is independently determined for each side of the MPP.

One of the three multipliers, which is used at a time for step-size adaptation, is dictated by the comparison between the instantaneous gradient magnitude and the region dividers. If the gradient magnitude is higher than σ_H, suggesting that the MPP is still far, the high multiplier is used for accelerating the MPPT. When the gradient magnitude becomes lower than σ_H but still higher than σ_L, indicating that the MPP is not far, the medium multiplier is used for reducing the step size and preventing the operating point from jumping over the MPP. After the gradient magnitude is lower than σ_L, showing that the MPP is near, the low multiplier is therefore used for avoiding the steady-state oscillation around the MPP [7]. Although the technique contributes to step-size adaptation, the suitable multiplier set is specific to the considered PV array. In addition, the befitting multipliers can be investigated by means of tests or simulations, which are tiring and time consuming. For more practical convenience, a step-size adaptation without multiplier is preferable.

4. PROPOSED STEP-SIZE ADAPTATION BASED ON POWER AND CURRENT VARIATION

An adaptive step-size scheme which eliminates optimum multiplier requirement, increases the tracking speed, and reduces the oscillation around the MPP, has been obtained

as a result of this research. Hereby, the adaptation of step size depends on changes in PV array output power and current. In this research, the step size describes the change in V_{pv} (ΔV_{pv}). The mathematical expression of step-size adaptation is derived as follows.

The array output power, P_{pv}, is calculated from

$$P_{pv} = V_{pv} I_{pv} \tag{3}$$

where, V_{pv} and I_{pv} refer to the array output voltage and current respectively. Calculation of the derivative of P_{pv} relative to V_{pv} provides

$$\frac{dP_{pv}}{dV_{pv}} = V_{pv} \frac{dI_{pv}}{dV_{pv}} + I_{pv} \tag{4}$$

After rearrangement of (4), it gives:

$$dV_{pv} = \frac{dP_{pv}}{V_{pv} \dfrac{dI_{pv}}{dV_{pv}} + I_{pv}} \tag{5}$$

The incremental conductance dI_{pv}/dV_{pv} should be restrained to prevent the steady-state fluctuation of the array voltage in the vicinity of the MPP, and hence to preserve the MPPT accuracy. Since the tracking direction is determined by the incremental conductance algorithm, only the magnitude of step size is required here. A desired step size (ΔV_{pv}^*) is then calculated from

$$\Delta V_{pv}^* = \frac{\left|\Delta P_{pv}\right|}{V_{pv} \left|\dfrac{\Delta I_{pv}}{\Delta V_{pv,\max}}\right| + I_{pv}} \tag{6}$$

where, $\Delta V_{pv,\max}$ refers to a maximum step size. According to (6), a change in PV power magnitude ($|\Delta P_{pv}|$) is big while the array operating point is distant from the MPP and becomes smaller as the array operating point gets closer to the MPP. Therefore, the array operating-point location with respect to to the MPP contributes to the step-size adaptation. In addition, the term $|\Delta I_{pv}/\Delta V_{pv,\max}|$ suits the step-size adaptation properly since the PV current is low whereas the array operating point is on the right of the MPP. This ratio increases the equation denominator. While the array operating point becomes closer to the MPP, low desired step size is therefore ensured to prevent jumping over.

4.1. PV System Using a Step-Up Converter for MPPT

Traditionally, a power converter has been used for maximizing the PV array power. A step-up converter was hereby selected for the MPPT procedure, and therefore located between the array and a battery bank which served as load of the system as indicated in Fig. 4. The battery bank was represented by a simple series connection model of a resistor R_b describing the battery internal losses and a capacitor C_b explaining the battery bank capacity. Based on the converter switching, the switch duty ratio affected the capacitor C_1 voltage which regulated the array voltage.

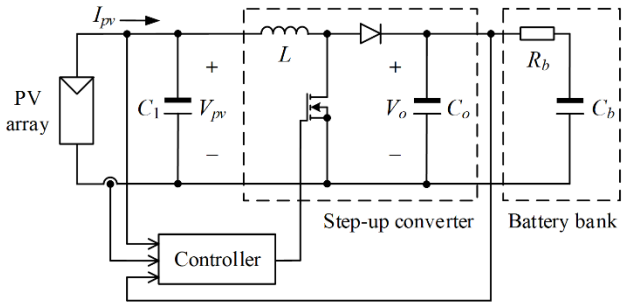

Fig. 4. Circuit diagram for step-up Converter based MPPT.

The required step size for MPPT, which corresponds to the desired change in PV array voltage (ΔV_{pv}^*), is controlled by the adaptation of converter duty ratio (ΔD). To accomplish the required alteration of array voltage, determination of the related adaptation of duty ratio is needed. On the basis of step-up converter voltage gain, the correlation between the array voltage and the output voltage of the converter (V_o) can be calculated from

$$V_{pv} = (1 - D) V_o \tag{7}$$

where, D refers to the converter duty ratio. The derivative of array voltage in (7) is expressed as

$$dV_{pv} = (1 - D) dV_o - V_o dD. \tag{8}$$

After reorganizing (8), the duty ratio variation (ΔD) related to ΔV_{pv}^* is shown as

$$\Delta D = \frac{(1 - D)\Delta V_o - \Delta V_{pv}^*}{V_o}. \tag{9}$$

According to (9), ΔD in the presented MPPT procedure is promptly obtained from the expected alteration of array voltage, and thus serves as the variable step size which engenders the array voltage variation until the MPP is found. In addition, if another converter is applied rather than the step-up converter, the ΔD and ΔV_{pv}^* correlation can be determined likewise. Furthermore, the battery serves as a load in this study, the converter output voltage, can be therefore considered essentially constant with respect to the converter switching frequency, and hence (9) can be simplified to

$$\Delta D = -\frac{\Delta V_{pv}^*}{V_o}. \tag{10}$$

By means of MATLAB simulation, the purposed step-size adaptation technique was then applied to the MPPT, and the resulting performance was compared with those

accomplished by the step-size adaptation using a multiplier set and by a fixed step-size scheme.

5. SIMULATION RESULTS AND DISCUSSION

The PV array output can be explained by an uncomplicated mathematical model irrespective of the series and parallel resistance components in the solar cell [5]–i.e.

$$I_{pv} = n_p I_{ph} - n_p I_o[\exp\{qV_{pv}/(n_s AkT)\} - 1] \quad (11)$$

where, I_{ph} and I_o are the photocurrent and the reverse saturation current of solar cell respectively, q is the charge of electron, A is the perfection factor of p-n junction, k is the Boltzmann's constant, and T is the temperature of solar cell, n_p is the number of parallel branches in the array, and n_s is the number of series cells in each branch.

The PV array considered in this simulation could generate the short-circuit current of 13.3 A, the open-circuit voltage of 240 V, and the maximum power of 2.27 kW under STC. The array power-voltage characteristics affected by irradiance and solar cell temperature are shown in Figs. 1 and 2 respectively. Referring to Fig. 4, parameters of the step-up converter and the battery bank were selected as follows: switching frequency = 20 kHz, C_1 = 4700 μF, L = 1 mH, C_o = 1000 μF; R_b = 0.5 Ω, and C_b = 47 F. Prior to the MPPT simulation with the multiplier-based step-size adaptation, the multiplier set suitable for the considered PV array specification had to be determined.

5.1. Investigation of the suitable multiplier set applied to a fixed step size

To determine the suitable multiplier set, the region dividers on the power-voltage curves for the three-multiplier scheme were beforehand specified. Since the maximum gradient magnitudes of the considered array power-voltage curve under STC ($|dP/dV|_{max}$) was about 12 W/V on the left side of the MPP and was about 120 W/V on the right side of the MPP, the region dividers for each side were calculated according to (1) and (2). Three carefully-chosen multiplier sets were investigated through MPPT simulation under specified rapid changes in weather conditions as shown in Fig. 5.

Determination of the suitable multiplier set was based on observation of transient behavior, namely overshoot, rising time, and settling time of the PV voltage. In addition to providing the least settling time, the low multiplier of each set was intentionally assigned to 1 in order to match the fix step-size scheme. The high multiplier of 5 gave less rising time than that of 3, but more than that of 8. Using the high multiplier of 5 together with the medium multiplier of 3, however, resulted in less overshoot. Therefore, the multiplier set of 1, 3, and 5 was considered suitable for the MPPT performance comparison with the purposed step-size adaptation technique.

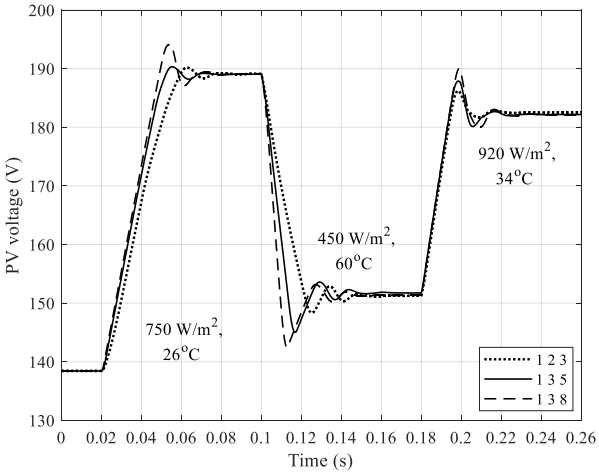

Fig. 5. MPPT using various multiplier sets for step-size adaptation.

5.2. Comparison of MPPT performance

The MPPT accomplished by the purposed step-size adaptation, the multiplier-based step-size variation, and the fixed step-size approach was carried out under hasty changes in environmental condition and reflected by the PV voltage variation as shown in Fig. 6. During this MPPT incident, the array operating point was relocated on the power-voltage curves as indicated in Fig. 7 and the PV output power fluctuation was indicated in Fig. 8.

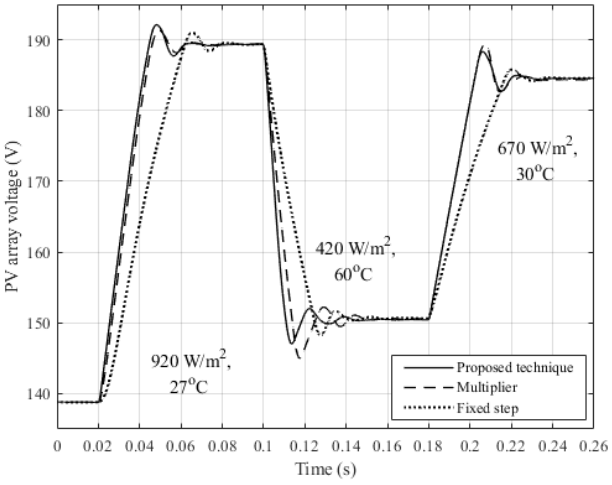

Fig. 6. Comparison of MPPT performance.

At first, the irradiance was 920 W/m^2, the solar cell temperature was 27˚C, and the initial duty ratio of the step-up converter caused the starting operating point to be located at the point "1" where the PV power of 1.68 kW was obtained. The MPPT was started at t = 20 ms, the duty ratio was lessened to boost the array voltage according to (10), hence the operating point was relocated to the current MPP (point "2") and the PV power was raised to 2.06 kW

(increased by 22.62%). In term of PV voltage with regard to MPPT performance relative to the fixed step-size approach, the purposed step-size adaptation and the multiplier-based step-size adaptation gave higher overshoot by 2.27% and 0.51% respectively, but less rising time by 41.43% and 37.67% respectively, and less settling time by 20.86% and 19.53% respectively. Despite giving higher overshoot, the purposed step-size adaptation provided less rising time and less settling time, compared with the multiplier-based step-size adaptation.

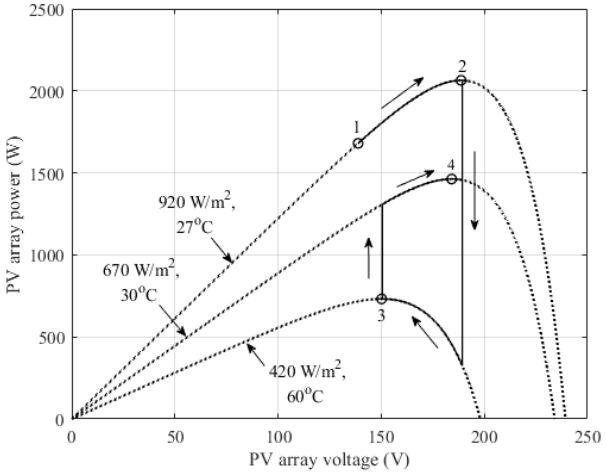

Fig. 7. Operating point movement during MPPT.

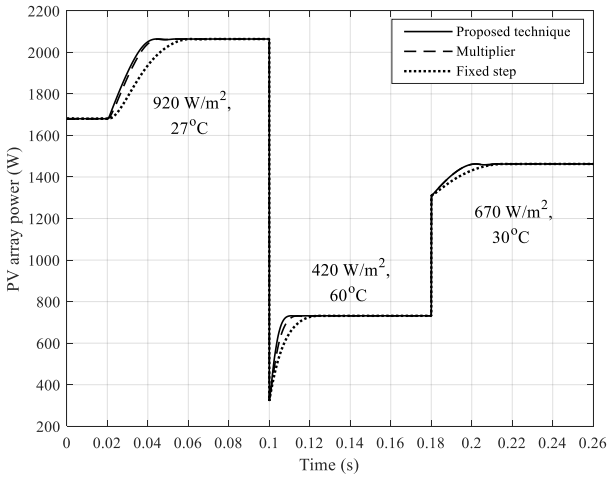

Fig. 8. PV power variation during MPPT.

When the irradiance dropped abruptly to 420 W/m^2 and the solar cell temperature went up to 60˚C at t = 0.1 s, the PV current declined suddenly while the PV voltage was supported by the capacitor C_1 and thus the PV power fell to 321.6 W. In response to this weather condition change, the system controller increased the converter duty ratio to reduce the PV voltage, and the operating point was moved to the new MPP (point "3") boosting the PV power to 731.7 W. In term of PV voltage with regard to MPPT performance compared to the fixed step-size approach, the purposed step-size adaptation and the multiplier-based step-size adaptation provided higher overshoot by 3.15% and 11.47% respectively, but less rising time by 56.45% and 45.08% respectively, and less settling time by 30.87% and 0.33% respectively.

At t = 0.18 s, the irradiance then rose suddenly to 670 W/m^2 and the solar cell temperature fell to 30˚C, the PV current increased rapidly as the PV voltage was held by the capacitor C_1 and therefore the PV power went up to 1.31 kW. In accordance to MPPT algorithm, a decrease in the converter duty ratio raised the array voltage, and hence the operating point was moved to the present MPP (point "4") raising the PV power to 1.46 kW. When compared to the fixed step-size strategy, the purposed step-size variation and the multiplier-based step-size variation gave higher overshoot by 7.43% and 11.12% respectively, but less rising time by 39.67% and 39.94% respectively, and less settling time by 10.07% and 9.37% respectively.

Regarding the multiplier-based step-size adaption, the choice of high multiplier value was necessarily limited to avoid high overshoot and prolonged oscillation around the MPP. Therefore, the resulting maximum step size could not be as big as the one obtained in the purposed algorithm. As the array operating point moved towards the MPP, the reduced step size using the medium multiplier gave consequently longer rising time. Since the step size was then kept constant in that middle region, the overshoot suppression tended to be less effective when finding the MPP. In contrast, the step size of the purposed technique was progressively adjusted while approaching the MPP and thus caused the PV voltage to change faster (less rising time). This gradual reduction of step size could also suppress the overshoot potentially and hence the PV voltage response reached its steady state faster (less settling time).

6. CONCLUSIONS

In this paper, the establishment of a step-size adaptation technique for maximizing the PV array output power based on PV power and current variation has been presented. The adaptive step size is subject to the array operating point position related to the existing MPP. The tracking direction is independently determined by the chosen MPPT algorithm, in which the incremental conductance method was adopted due to capability of handling MPPT under fast change in weather conditions. While tracking the MPP, the duty ratio of the power converter is progressively adjusted in correspondence to the desired step size. This adaptive scheme provides therefore higher tracking speed and reduction of steady-state fluctuation in the vicinity of the MPP. In addition, the purposed technique is independent of PV array specification, and thus complexity of suitable multiplier investigation for each PV array as implemented

in the multiplier-based step-size adaptation method is avoided. The proposed step-size adaptation contributes to succeeded MPPT procedure during rapid change in weather conditions with superior performance when compared with the multiplier-based step-size adaptation and the fixed step-size strategy.

ACKNOWLEDGEMENTS

The authors are grateful to the Faculty of Engineering, Naresuan University for supporting this research financially and also providing research facilities.

REFERENCES

[1] Hille, G.; Roth, W.; and Schmidt, H. 1995. Course book for the seminar - Photovoltaic Systems. Freiburg: Fraunhofer Institute for Solar Energy Systems.

[2] Trabelsi, H.; Elloumi, M.; Abid, H.; and Kharrat, M. 2017. MPPT controllers for PV module panel connected to grid. In *Proceedings of the 2017 18th International Conference on Sciences and Techniques of Automatic Control and Computer Engineering*. Monastir, Tunisia, 21-23 December. New York: Institute of Electrical and Electronics Engineers.

[3] Benkercha, R.; Moulahoum, S.; and Colak, I. 2017. Modelling of fuzzy logic controller of a maximum power point tracker based on artificial neural network. In *Proceedings of the 2017 16th IEEE International Conference on Machine Learning and Applications*. Cancun, Mexico, 18-21 December. New York: Institute of Electrical and Electronics Engineers.

[4] Uddin, M. H.; Baig, M. A.; and Ali, M. 2016. Comparision of 'perturb & observe' and 'incremental conductance', maximum power point tracking algorithms on real environmental conditions. *In Proceedings of the 2016 International Conference on Computing, Electronic and Electrical Engineering*. Quetta, Pakistan, 11-12 April. New York: Institute of Electrical and Electronics Engineers.

[5] Hussein, K. H.; Muta, I.; Hoshino, T.; and Osakada, M. 1995. Maximum photovoltaic power tracking: an algorithm for rapidly changing atmospheric conditions. *IEE Proceedings - Generation, Transmission and Distribution*, 142(1): 59-64.

[6] Belkaid, A.; Gaubert, J.-P.; and Gherbi, A. 2017. Design and implementation of a high-performance technique for tracking PV peak power. *IET Renewable Power Generation*. 11(1): 92-99.

[7] Lousuwankun, P. and Jantharamin, N. 2020. Maximum power point tracking with step size variation using multiplication factor. In *Proceedings of the The 43rd Electrical Engineering Conference.* Phitsanulok, Thailand, 28-30 October. Bangkok: Electrical Engineering Academic Association (Thailand).